

Physically based and neuro-fuzzy hybrid modelling of thermomechanical processing of aluminium alloys

M.F. Abbod^{a,b}, D.A. Linkens^{a,b,*}, Q. Zhu^{a,c}, M. Mahfouf^{a,b}

^a *IMPETUS, Institute for Microstructural and Mechanical Process Engineering, The University of Sheffield, Sheffield, UK*

^b *Department of Automatic Control and Systems Engineering, University of Sheffield, Mappin Street, Sheffield S1 3JD, UK*

^c *Department of Engineering Materials, University of Sheffield, Sheffield S1 3JD, UK*

Received 29 June 2001; received in revised form 25 October 2001

Abstract

Modelling of the microstructural evolution of aluminium alloys during thermomechanical processing is a desirable method for predicting the alloy's properties and designing the process variables to achieve the desired goals. A dynamic model has been developed in terms of the internal states variables of the process comprising the dislocation density, the subgrain size, and the misorientation between the subgrains. The developed model is based on a hybrid modelling technique known as grey-box modelling where intelligent models and physical equations are merged to predict the material properties with respect to the deformation conditions. The model predicts the evolution of the internal states variables under transient deformation conditions, as well as the static subsequent recrystallisation behaviour, nucleation of recrystallisation based on experimental results and quantitative metallurgical observations. In the model, the flow stress and recrystallisation behaviour are predicted with respect to temperature, strain rate and strain for different aluminium alloys providing a reasonable agreement with experimental data. © 2002 Elsevier Science B.V. All rights reserved.

Keywords: Aluminium alloys; Microstructure modelling; Internal state variables; Recrystallisation; Neuro-fuzzy models; Physically based models

1. Introduction

Modelling of microstructural evolution of aluminium alloys during thermomechanical processing such as forging, rolling or extrusion is an attractive method to predict the material properties. Composition of the materials, deformation strain, strain rate and temperature are the key variables which change from one material to another and from one type of processing to another. For aluminium alloys, changes in the deformation conditions affect the evolution of dislocation substructure and subsequent recrystallisation.

A hybrid technique such as semi-physical modelling provides a good tool that combines different modelling approaches in one dynamical model [1]. Combinations of physically based models and intelligent (neuro-fuzzy) models work very efficiently. While the physical model

ensures that the results are physically sensible, the neuro-fuzzy model can be utilised to increase the accuracy of the results. One of the hybrid grey-box modelling techniques is the 'hybrid' semi-parametric model which utilises serial and parallel parametric and non-parametric models and gives advantages for compensating for sparse data, extrapolation improvements, uncertainty and the bias of the default model.

In this paper, the hybrid semi-physical model which has been developed is based on the internal state variables of the material being processed. The internal state variables are dislocation density (ρ_i), subgrain size (δ) and misorientation between subgrains (θ) [2]. The dislocation density consists of two parts; the so-called 'random' and 'geometrically necessary' components. The internal state variables and subsequent recrystallisation behaviour are developed for constant and transient deformation conditions which cover a wide temperature range for different aluminium alloys. The model predicts the evolution of the internal state variables in transient deformation, the final flow stress, the nucle-

* Corresponding author. Tel.: +44-114-222-5133; fax: +44-114-222-5614.

E-mail address: d.linkens@shef.ac.uk (D.A. Linkens).

ation density of recrystallisation (N_v), the recrystallisation kinetics (t_{50}) and the recrystallised grain size (d_{rex}).

Using the neuro-fuzzy technique the dynamic evolution of the internal state variables has been modelled which has been applied to hot deformation of different aluminium alloys (Al, Al–1% Mg, Al–5% Mg, Al–11% Zn) covering a temperature range of 300–600 °C and strain rate range ($0.1–25 \text{ s}^{-1}$) during constant, increasing and decreasing strain rate deformation. The internal state variables are fed to parametric model blocks which calculate the final stress and the recrystallisation behaviour. Any misfit in the final stress is compensated by a parallel non-parametric model that calculates the friction stress due to the solution hardening during deformation as shown in Fig. 1. Simulation results are presented and compared to the original data to give an indication of the model accuracy.

2. Semi-physical modelling

The basic principle of transforming the black-box from ‘opaque’ to ‘translucent’ is to incorporate physical knowledge about the process being modelled into the box. Parametric models (white-box models) are based on first-principles and therefore can be used to predict not only the process behaviour, but also have the capability to explain the underlying physical and chemical relationships of the process. The models should be sustained with experiments to estimate some of the process parameters. White-box models can be used for different process conditions, but experiments are necessary since some parameters are not easy to express in a simple way as a function of the process characteristics.

In contrast, non-parametric models (black-box models) are often used to represent systems for identification and subsequent modelling and control. The parameters of such models are estimated from the system input-output data, using standard techniques. In fact, such parameters may be functions of known physical parameters of the underlying dynamic system. If such parameters were known physically, the transfer function of the model can be deduced without the need

for identification. As a disadvantage, black-box models can only be used in the operating regime for which they are identified.

Combining prior physical knowledge with black-box modelling provides a better approach to modelling. Two different approaches can be distinguished. When the basic modelling frame is a black-box, then it is known as ‘grey-box modelling’ [3,4]. On the other hand, when the model is based on first-principles (white-box model) and then includes black-box elements as part of the white-box model frame, this method is known as ‘hybrid modelling’ or ‘semi-physical modelling’ [5].

2.1. Takagi–Sugeno–Kang auto regressive model (TSK-ARX)

The Takagi–Sugeno–Kang (TSK) method of expressing fuzzy rules [6] has fuzzy sets in the premise part and a regression model as the consequent in the form:

$$\text{IF } x_1 \text{ is } B^1 \text{ and...and } x_n \text{ is } B^n \\ \text{THEN } y = c_0 + c_1x_1 + \dots + c_nx_n, \tag{1}$$

where $x = (x_1, \dots, x_n)^T$ and y are the input and output linguistic variables, while B^i and C are the linguistic values characterised using membership functions. Since this form of rule representation contains more information, the number of rules required will typically be much less than for relational fuzzy models. A complex high dimensional non-linear modelling problem is decomposed into a set of simpler linear models valid within certain operating regions defined by fuzzy boundaries. Fuzzy inference is then used to interpolate the outputs of the local models in a smooth fashion to get a global model. This model approach provides a better modelling accuracy than relational fuzzy models.

Consider a single input–single output (SISO) system which can be modelled using the method proposed by TSK. Assuming the input space is partitioned using p fuzzy partitions and that the system can be represented by fuzzy implications (one in each fuzzy sub-space), the model can be written as follows:

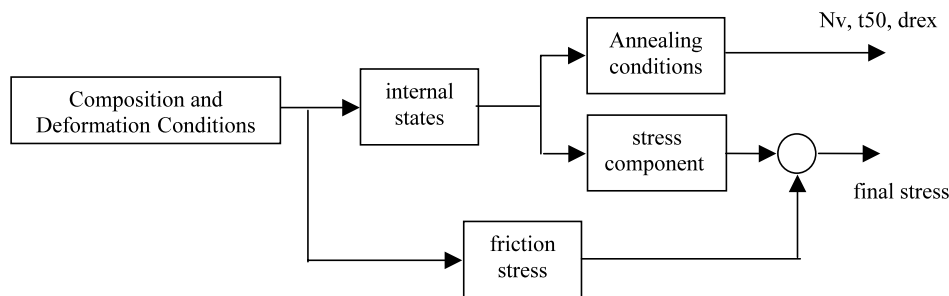


Fig. 1. Block diagram of the microstructure grey-box model.

L^i : IF $y(t)$ is B^i

THEN $y_m(t + 1)$
 $= a^i_1 y(t) + \dots + a^i_j y(t - j + 1) + b^i_1 u(t) + \dots$
 $+ b^i_j u(t - j + 1) + k_i,$ (2)

where $y(t)$ and $u(t)$ are the process inputs and outputs at time t , $y_m(t + 1)$ is the one step ahead model prediction at time t , B^i is a fuzzy set presenting the fuzzy sub-space in which implementation L^i can be applied for reasoning, k_i is a term that accounts for offset and $i = 1, \dots, p$.

The model parameters can be realised by auto-regression and can be expressed in the following matrix form:

$$\Theta = \begin{bmatrix} a^1_1 \dots a^1_{n_a} & b^1_1 \dots b^1_{n_a} \\ \vdots & \vdots \\ a^p_1 \dots a^p_{n_a} & b^p_1 \dots b^p_{n_a} \end{bmatrix} \quad (3)$$

The overall fuzzy model output can be written as:

$$y_m(t + 1) = \beta \Theta \Phi(t), \quad (4)$$

where:

$$\Phi(t) = [-y(t), -y(t - 1), \dots, -y(t - n_a + 1), u(t), u(t - 1), \dots, u(t - n_a + 1)],$$

$$\beta = [\beta_1 \beta_2 \dots \beta_i \dots \beta_p], \quad (5)$$

and

$$\beta_i = \frac{B^i[y(t)]}{\sum_{i=1}^p B^i[y(t)]}, \quad (6)$$

where $B^i[y(t)]$ is the grade of membership of $y(t)$ in B^i and β is a vector of the weights assigned to each of the p implications at each sampling instant [7].

3. Hot deformation behaviour of aluminium alloys

3.1. Modelling of material properties

A promising approach for modelling material properties is to include the internal state variables of the process as well as the inputs and outputs. The output parameters are the flow stress (σ), the density of nuclei for recrystallisation (N_v) and the average growth rate for recrystallisation (\bar{G}) which can be related to the internal state variables and the values for the external variables of strain rate ($\dot{\epsilon}$) and temperature (T) [8] as:

$$\sigma = f(T, \dot{\epsilon}, S_1, \dots, S_n) \quad (7)$$

$$N_v = f'(T, \dot{\epsilon}, S_1, \dots, S_n) \quad (8)$$

$$\bar{G} = f''(T, \dot{\epsilon}, S_1, \dots, S_n), \quad (9)$$

where S_1, \dots, S_n are the material parameters such as the internal state variables, material composition, pre-treatments conditions etc., with the evolution equation for the internal state variables which is determined by:

$$S_j = g(T, \dot{\epsilon}, S_1, \dots, S_n), \quad (10)$$

where S_j is a microstructural characteristic such as ρ_i , δ , θ , d_{rex} etc.

In thermomechanical processing, the strain rate and temperature, which can be described by the Zener–Hollomon parameter $Z = \dot{\epsilon} \exp(Q/RT)$, where Q is the activation energy, generally change continuously during the deformation process itself and may change from one pass to another.

Modelling of the flow stress is carried out in terms of the internal state variables ($\rho_i^{-1/2}$, δ , θ) which in turn are determined by the deformation conditions (T , $\dot{\epsilon}$, ϵ). The final flow stress (σ) is the sum of the effective stress (σ_e) (known as friction stress (σ_f) [2]) and the internal stress (σ_i) that arises from microstructure [9] as shown in Eq. (11)

$$\sigma = \sigma_e + \sigma_i \quad \sigma_i = \sigma_{\rho_i} + \sigma_{\delta} + \sigma_d + \sigma_p, \quad (11)$$

where σ_{ρ_i} is the stress due to interaction of dislocations inside the subgrain, σ_{δ} is the long range internal back stress due to subgrain boundaries, σ_d is the stress arising from grain boundaries, and σ_p is the stress due to second phase particles.

In single phase polycrystals with large grains compared to subgrains which undergo only recovery processes such as for aluminium alloys, the terms σ_p and σ_d can be neglected and the internal stress is mainly the sum of σ_{ρ_i} and σ_{δ} . Therefore the final flow stress during deformation involves stresses arising from internal dislocations (σ_{ρ_i}), from subgrain boundaries (σ_{δ}) and the friction stress arising from glide of internal dislocations (σ_f) as [10]:

$$\sigma_{\rho_i} = \alpha_1 M G b \rho_i^{1/2}, \quad (12)$$

$$\sigma_{\delta} = \alpha_2 M G b / \delta, \quad (13)$$

$$\sigma_f = \frac{M B}{D_0 b^2} \frac{Z}{\rho_m}, \quad (14)$$

where $\alpha_1 = 0.38$ and $\alpha_2 = 0.79$ for aluminium alloys are constants, $M = 3$ for fcc polycrystals is the Taylor factor, $D_0 = 1$ is the diffusion frequency, $G = (29484 - 13.6T)$ MPa is the shear modulus, $b = 0.286 \times 10^{-9}$ m is the Burgers vector, ρ_m is the mobile dislocation density, which is the same order of magnitude as the internal dislocation density ρ_i for hot deformation at constant strain rate, and B is a material constant reflecting solution hardening.

The internal state variables of the process during deformation can be written in exponential form [11]:

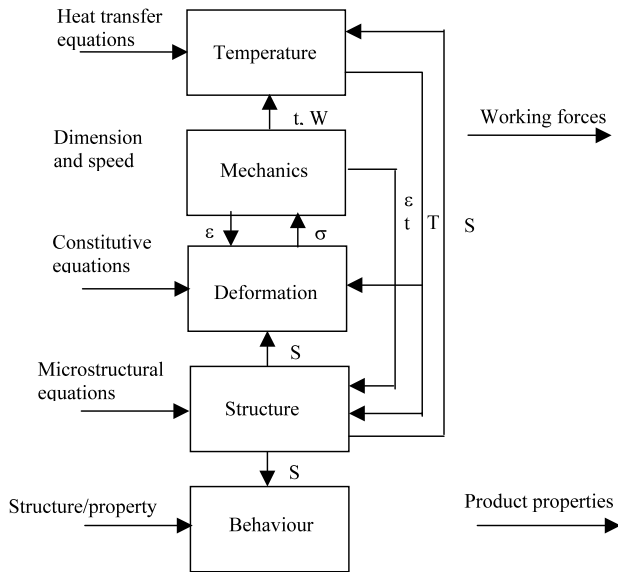


Fig. 2. Schematic diagram of the hot forming process (t , time; W , working forces; T , temperature; S , internal states; σ , stress; ϵ , strain).

$$S_j = S_{j0} + (S_{js} - S_{j0}) \left[1 - \exp\left(-\frac{\epsilon}{\epsilon_{sj}}\right) \right]$$

$$S_j = \rho_i^{1/2}, 1/\delta, \theta. \quad (15)$$

The overall model is based on the evolution of microstructure in a thermomechanical environment. It includes modelling the mechanics and heat transfer conditions to provide input data for the microstructural model as shown in Fig. 2. The model must involve microstructure/properties relationships that are used interactively to compute the product properties. It should also allow for inner variables examination and optimise the process conditions within the constraints imposed by the plant.

The internal dislocation density consists of two parts, the so-called 'random' dislocation density (ρ_r) and 'geometrically necessary' dislocation density (ρ_g), $\rho_i = \rho_g + \rho_r$. The random dislocation density produces homogeneous strain and the geometrically necessary dislocations are related to subgrain boundaries which contribute the local curvature. For deformation at constant strain rate and temperature in commercial Al–Mg alloys, $\rho_g \approx 0$, i.e. $\rho_i \approx \rho_r$. However, for transient deformation, ρ_g is of greater significance in describing the evolution of internal dislocation density. Unlike ρ_r , which contributes both to local stored energy and to flow stress, ρ_g mainly contributes to the total stored energy but little to the flow stress [2]. This is due to the fact that the material being described is not heat treatable which means that the second phase hardening are negligible, consequently the geometrically necessary dislocations are negligible for constant strain rate. On the other hand, they have a significant value for changing strain rate and they mainly contribute to the stored energy and subsequent recrystallisation behaviour [12].

For constant strain rate deformation the evolution of the dislocation density does follow the designed model [11]. For decreasing strain rate, however, the calculated data are lower than the experimental data during changing strain conditions [10]. This means that the required model is more complex for changing strain rate deformation conditions.

For decreasing strain rate, the subgrain size follows the evolution law of Eq. (15) for constant strain rate until it reaches its minimum value. Then there is a rapid increase in the subgrain size. This arises from dissolving subgrain boundaries which leaves excess dislocations in the subgrain interior and increases the total internal dislocation density. These dislocations from the dissolved subgrain boundaries are the so-called 'geometrically necessary' internal dislocations. The evolution of the subgrain size has mostly been studied at relatively large strain (steady state). Exponential equations have been used to model the evolution of subgrain size and misorientation between subgrains at constant strain rate and temperature. For changing strain rate deformation, the resultant data deviate from the experimental data using exponential equations [10]. This means that the equations are not sufficient to predict the evolution of dislocation structure.

Total curvature ($1/R$) is a key parameter for nucleation of recrystallisation which is determined by geometrically necessary dislocations and subgrain boundary as:

$$\frac{1}{R} = \rho_g b + \frac{\theta}{\delta} \quad (16)$$

As discussed above, for constant strain rate deformation $\rho_g \approx 0$, i.e. $1/R \approx \theta/\delta$.

3.2. Stress–strain relationship

A collection of experimental data on dislocation structure evolution and deformation kinetics of some aluminium alloys at elevated temperatures is available from the literature [13]. Fig. 3 shows the stress–strain curves of torsion tests for different aluminium alloys at 300 °C and 1.0 s⁻¹. Al has the lowest flow stress. Al–11% Zn resembles Al in the steady-state range but has higher transient stress due to weak solid solution hardening. Al–1% Mn has intermediate deformation resistance but still resembles the behaviour of Al, i.e. the stress increases with strain to a plateau steady-state value. Alloys of the Al–5% Mg type exhibit the highest deformation resistance due to strong solid solution hardening being responsible for the fast rise in stress and stress increases with strain to a peak value followed by a decrease. Detailed analysis [13] shows that this arises from deformation heating and geometric dynamic recrystallisation, rather than the traditional dynamic recrystallisation. Therefore, the evolution laws of dislo-

cation substructures derived by recovery theory (Eq. (15)) are qualitatively the same for Al and Al–Mg alloys.

The maximum flow stress (steady state) are taken as an approximate measure of the steady-state flow resistance and plotted in Fig. 4 in a normalised manner. The influence of the temperature T was compensated by

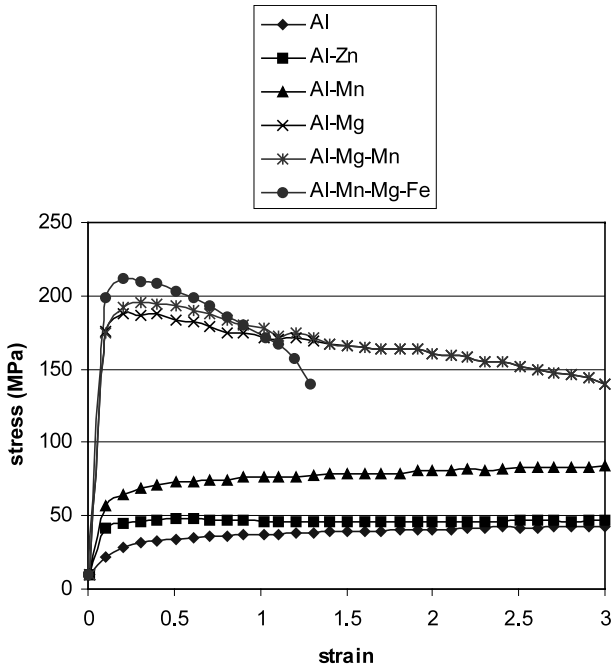


Fig. 3. Stress–strain curves for different alloys deformed at 300 °C and 1.0 s⁻¹.

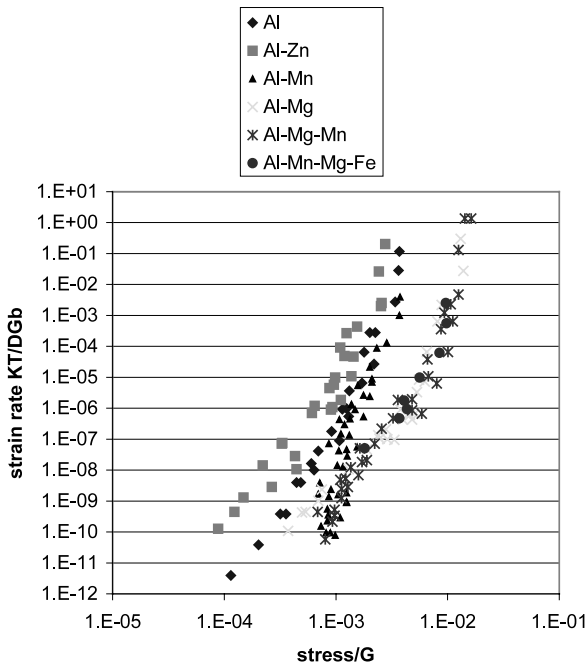


Fig. 4. Stress–strain relationship for different material compositions.

dividing the stress by the shear modulus (G) of aluminium, and multiplying the strain rate by the expression (kT/DGb) where k is the Boltzmann constant, and D is the diffusion coefficient. Two groups can be classified, the first being an Al–Mg group, while the second is an Al group.

Based on Fig. 4, three-dimensional (3D) surfaces were generated for four types of composition, namely Al, Al–11% Zn, Al–5% Mg, Al–1% Mg as shown in Fig. 5. The 3D surface represents the final stress as a function of temperature and strain rate based on a neuro-fuzzy model

$$\text{stress} = f(\text{temperature, strain rate}). \tag{17}$$

The effect of the Mg percentage was taken into account when calculating the final flow stress [14]. Fig. 6 shows the stress as a function of magnesium content for deformation at 385 °C to strain of unity.

The internal state variables have also been obtained for the same alloys [2]. The characteristic steady-state dislocation spacings are displayed as a function of stress/ G in Figs. 7 and 8, i.e. spacing between internal dislocations ($\rho_i^{-1/2}$), spacing between subgrain boundaries, i.e. subgrain size (δ) and spacing between sub-boundary dislocations (S) which is related to subgrain boundary misorientation as $S \approx b/\theta$.

Another component that contributes to the final stress is the friction stress which is un-measurable. It can, however, be calculated from Eq. (11) by working out the difference between the final measured stress and the summation of the stresses due to the internal state variables.

The steady-state internal state variables can be calculated as a function of temperature and strain rate for each of the alloys under the steady-state stress based on a non-linear neuro-fuzzy model as follows:

$$\text{Stress} = f(\text{temperature, strain rate}), \tag{18}$$

$$\text{Internal States} = f(\text{stress}). \tag{19}$$

Fig. 9 shows the internal state variables as a function of temperature and strain rate for Al–1% Mg. The temperature range for the relationships is chosen to be in the range of 300–600 °C, while the strain rate is chosen to be in the range of 0.1–25 s⁻¹. The final stress can be calculated by summing all the components of the internal stresses and the friction stress.

4. Modelling of recrystallisation behaviour

Nucleation of recrystallisation takes place in different places within a deformed material. A generalised model to relate the internal state variables and their distribution has been proposed recently [2] and is described by the following equation:

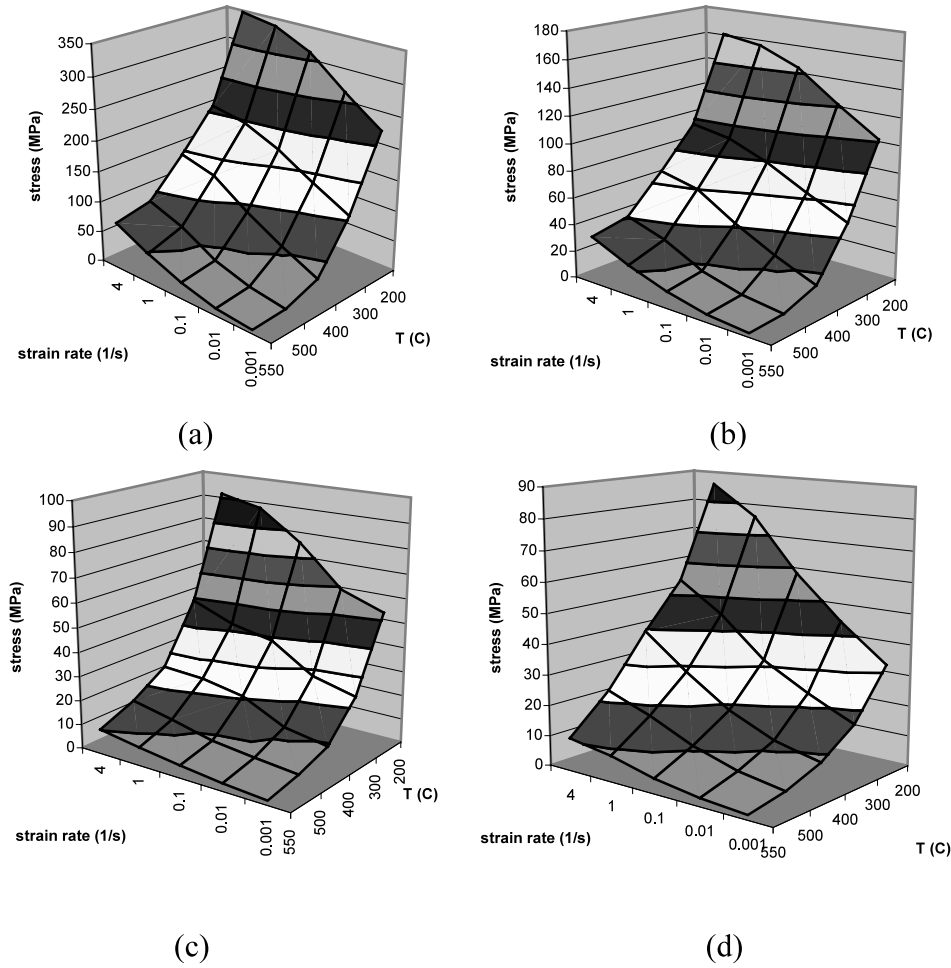


Fig. 5. Steady-state stress as a function of strain rate and temperature for: (a) Al–5% Mg; (b) Al–1% Mg; (c) Al; and (d) Al–11% Zn.

$$N_V = p_1\lambda_1P_V + p_2\lambda_2 \frac{L_V}{\delta} + p_3\lambda_3 \frac{S_V}{\delta^2} + p_4\lambda_4 + \frac{P_\theta}{\delta^3}, \quad (20)$$

where P_V is the number of grain corners per unit volume, and L_V is the line length per unit volume, for plane strain compression test (PSC) $L_V = 1.513[\exp(\varepsilon/1.155) + 0.5(1 + \exp(-(\varepsilon/1.155)))] \cdot d_0^{-2}$ S_V is the grain boundary surface area per unit volume. For PSC, $S_V = (0.429 \exp(-\varepsilon/1.155) + \exp((\varepsilon/1.155) + 0.571)) \cdot d_0^{-1}$. P_θ is the probability of finding mobile sub-boundaries, λ_1 – λ_4 are geometrical parameters and p_1 – p_4 are the probabilities for finding subgrains with a size larger than a critical value that can provide the nuclei for recrystallisation related to the four different sites.

As the strain regime covers a wide range of thermomechanical processing conditions and the grain boundaries are the most significant places for nucleation, the equation can be simplified to:

$$N_V \approx p_3\lambda_3 \frac{S_V}{\delta^2} \quad (21)$$

where d_0 is the original grain size and p_3 can be assumed as a constant [2,15].

Recrystallisation kinetics is determined by both nucleation density and growth rate of nuclei. If the nucleation is site-saturated, which is a reasonable approximation after hot deformation, then the following kinetics law of recrystallisation is obtained:

$$X(t) = 1 - \exp(-X_{\text{ext}}(t)), \quad (22)$$

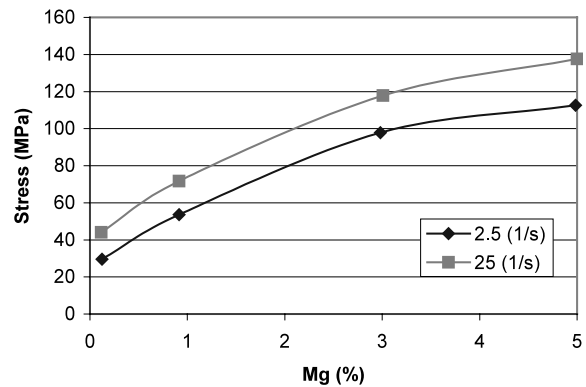


Fig. 6. Stress at a strain of unity as a function of magnesium contents for deformation at 385 °C.

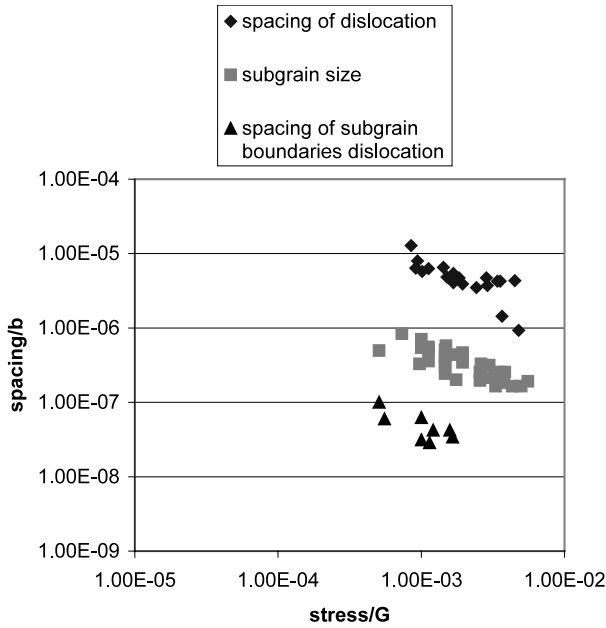


Fig. 7. Characteristics spacing of internal state variables at steady-state deformation for Al–Mg alloy group.

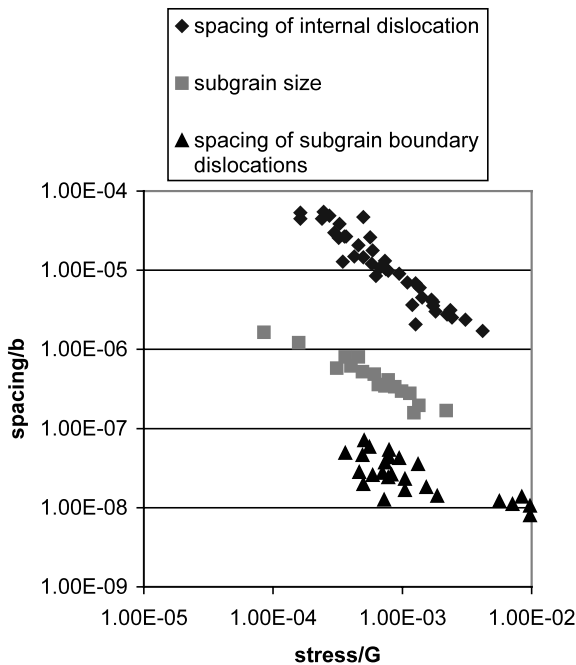


Fig. 8. Characteristics spacing of internal state variables at steady-state deformation for Al alloy group.

where $X(t)$ is the fraction recrystallised after annealing time t and $X_{\text{ext}}(t)$ is the corresponding extended volume which is determined by:

$$X_{\text{ext}}(t) = \frac{3}{4} \pi N_V (G_r \cdot t)^3, \quad (23)$$

where G_r is the growth rate of the recrystallisation nuclei which is mainly affected by the recovery from the

deformed microstructure and the spatial distribution of the stored energy on the scale of the grain size which is the same as that calculated from experimental results of the internal dislocation structure and statistical analysis [16] and is related to the stored energy (P_D).

$$G_r = M_{\text{gb}} P_D, \quad (24)$$

where M_{gb} is the grain boundary mobility.

The stored energy is calculated by:

$$P_D = \frac{Gb^2}{10} \left[\rho_i (1 - \ln(10b\rho_i^{1/2})) + \frac{2\theta}{b\delta} \left(1 + \ln\left(\frac{\theta_c}{\theta}\right) \right) \right], \quad (25)$$

where θ_c is the critical angle for distinguishing between a grain and subgrain boundary (approximately 15°).

The time for 50% recrystallisation can be calculated by the following equation:

$$t_{50} = C_3 P_D^{-1} N_V^{-1/3}, \quad (26)$$

where C_3 is a temperature-dependent material constant.

For site-saturated nucleation, the recrystallised grain size is simply calculated from the nucleation density as:

$$d_{\text{rex}} = AN_V^{-1/3}, \quad (27)$$

where A is a geometric parameter to relate the surface linear intercept size and spatial diameter of the grains. For grain structure of tetrakiadecahedra (TKD), $A = 0.2347$ [2].

5. Model developments

5.1. Internal states evolution

The dynamic evolution of the internal states has been modelled using the TSK-ARX technique described in Section 2 which has been applied to hot deformation of Al–1% Mg alloy during constant, increasing and decreasing strain rate in plane strain compression (PSC) tests.

Developing a dynamic TSK model is usually based on selecting the number of clusters for the training data, then based on the model complexity, the model order has to be selected together with a time delay. The more complex the model is, the higher the order of the model has to be selected. For the time delay, it is based on the data-sampling rate and the pure time delay in the system. Accordingly, a third order model with a unit delay has been developed for each internal state. Four models were generated, two for the random and geometrically necessary dislocation density, the subgrain size and the misorientation. Depending on the complexity of each model, the number of clusters (partitions) was selected independently. Since the strain-rate profile plays a vital role in the evolution of the internal state variables, the developed model was designed to be

based on three inputs, namely strain, strain rate, and the strain rate profile (constant, decreasing and increasing). Sample results for modelling the total internal dislocation density, subgrain size and misorientation for a constant strain rate (2.5 s^{-1}) are shown, respectively, in Fig. 10. The solid line is the modelled output, while the dotted points are the experimental data.

The effects of temperature and strain rate on the actual final steady-state values for the internal state variables are derived from the relationship of the internal state variables temperature and strain rate for each material composition. Based on the two classified groups (Al group, and Al–Mg group), the steady-state levels of the internal state variables are calculated and utilised to scale the dynamic behaviour of each internal state variable for the selected composition with respect to the temperature and strain rate.

After the internal state variables have been calculated, the stress due to each individual state can be calculated and summed together to calculate the final stress. Nevertheless, there is the friction stress which is another component to be added to the final stress. The friction stress is not measurable and therefore it is estimated as the difference between the final stress (measured) and the summed stress due to the internal states. The friction

stress is calculated and modelled for each composition as a function of temperature and strain rate.

5.2. Assembling the model

The model has been developed into block diagram from TSK-ARX and physically based models as shown in Fig. 11 and implemented in MATLAB/SIMULINK environment as shown in Fig. 12. The model consists of four stages. The first stage is the strain and strain-rate profile generator. The strain and strain rate are fed to the second stage (TSK-ARX) which calculates the internal state variables. The third stage is the summation of the internal state variables depending on the strain rate profile to generate the total values for the internal state variables. The internal state variables are fed to the final stage which consists of three blocks, the friction and final stresses blocks which calculate the friction stress and the internal stresses, while the other block calculates the static recrystallisation behaviour.

The main model inputs are the composition, temperature, strain rate and strain. The model calculates the internal state variables, the final flow stress and the recrystallisation behaviour (N_v , d_{rex} , t_{50}). Since the model covers a wide range of temperature and strain

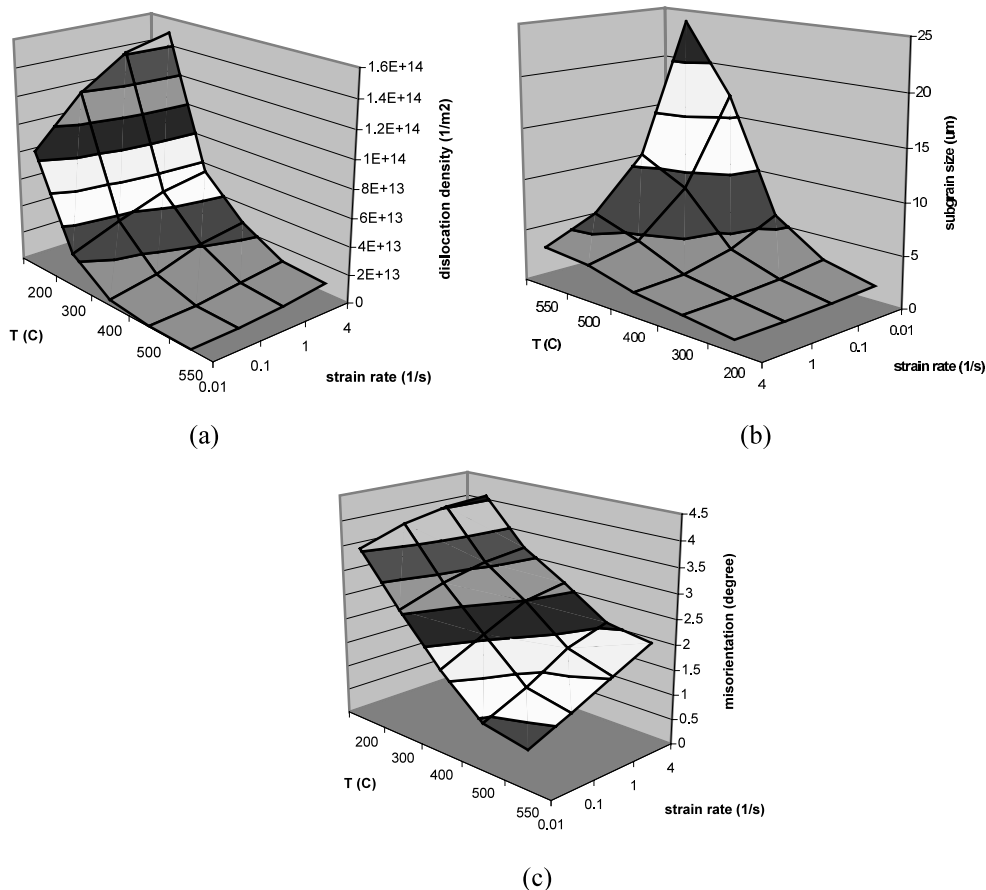


Fig. 9. Steady-state internal state variables for: (a) Al–1% Mg; (b) dislocation density; (c) subgrain size; and (d) misorientation.

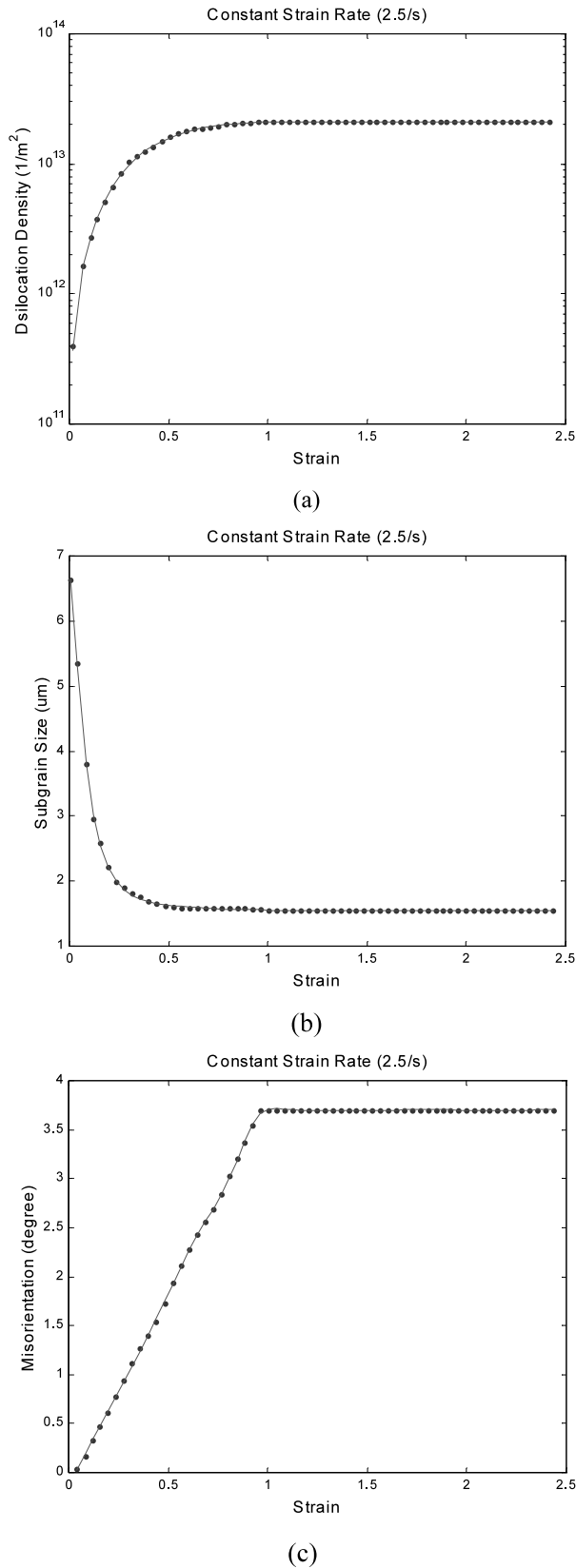


Fig. 10. Experimental and TSK-ARX model predicted internal states: (a) dislocation density; (b) subgrain size; and (c) misorientation.

rate for each individual composition, tuning the model was important to adjust some of the parameters for scaling the internal state variables and calculating the individual internal stresses.

6. Modelling results

6.1. Genetic algorithm optimisation

A genetic algorithm (GA) [17] was used to search for the best-fit parameters that scale the internal state variables and the parameters for calculating the individual stress components (α_1 and α_2 in Eqs. (12) and (13)). These five parameters were optimised using a multi-objective (recursive least square error, positive error) to minimise the error between the predicted stress and the measured stress. The GA was set to have population size of 10 for 100 epochs with average multi-objective ranking [18].

The model was optimised for a temperature range of 300–600 °C, strain rate within the range 0.1–25 s⁻¹ and strain range in the limits of 0–3. Four compositions were selected (Al, Al–1% Mg, Al–5% Mg, Al–11% Zn).

6.2. Simulation results

Simulation results were obtained for the four compositions by varying the temperature (300, 400, 500 and 600 °C) depending on the available measured stress data. Four levels for the strain rate were selected (0.1, 1, 2.5 and 25 s⁻¹). For each case the stress was calculated for a strain rate covering four temperatures. The same calculation was performed for the recrystallisation nucleation density, the kinetics and the recrystallised grain size. This has been performed for each individual composition. Figs. 13 and 14 show the simulation results for an Al–1% Mg composition showing the final stress (predicted, continuous lines; measured, points) and d_{rex} . The model has accurately predicted the flow stress for the trained data as well as for the recrystallisation conditions.

7. Conclusions and future work

This work has been done in collaboration with metallurgists whose knowledge and data have provided a good source for model building and the associated validation process. Although the model has been developed on a limited number of data points, it has shown good prediction accuracy which is due to the utilisation of the neuro-fuzzy modelling approach which facilitates the developments of good models based on small number of data. For grey-box modelling, the neuro-fuzzy

modelling technique provides good models which are based on the dynamics of the process. The transparent characteristics of those models allow the internal rules to be viewed, which makes it more suitable for the grey-box modelling approach.

The model developed so far is limited in its input space. The input space for the current model is based on strain, strain rate, temperature and four types of alloy compositions. For future work, expansion of the generalisation properties of the model will be undertaken to include further alloy compositions.

In further work the grey-box model has been integrated into a finite elements package and utilised for

calculating the stress and temperature distribution for rolling and PSC tests. Other variables can also be calculated and displayed on the final specimen mesh such as the internal states and the post-processing recrystallisation behaviour.

Acknowledgements

The authors gratefully acknowledge the Engineering and Physical Sciences Research Council, UK for their financial support under grant no. GR/L50198.

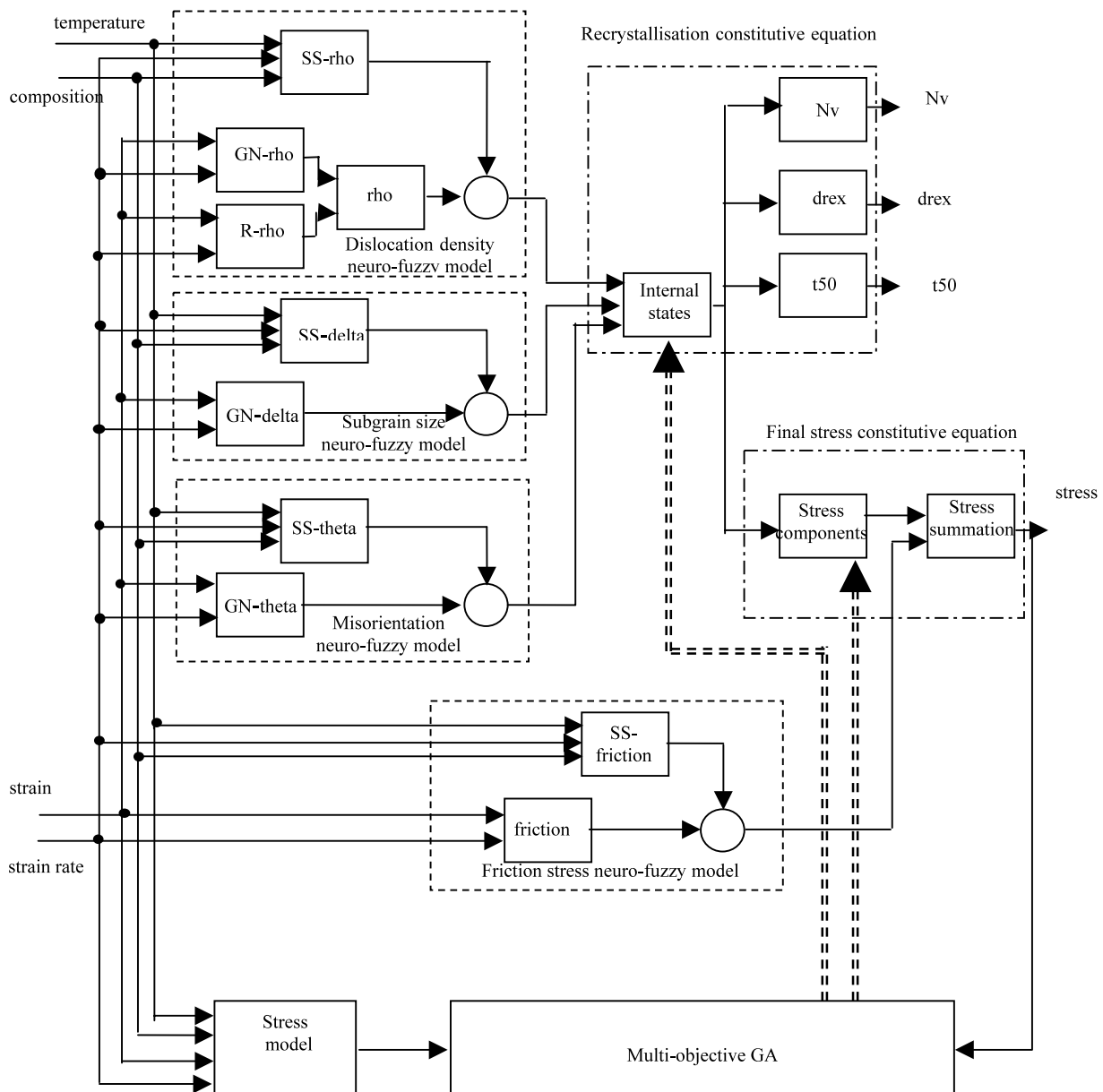


Fig. 11. Schematic diagram of the hot forming process.

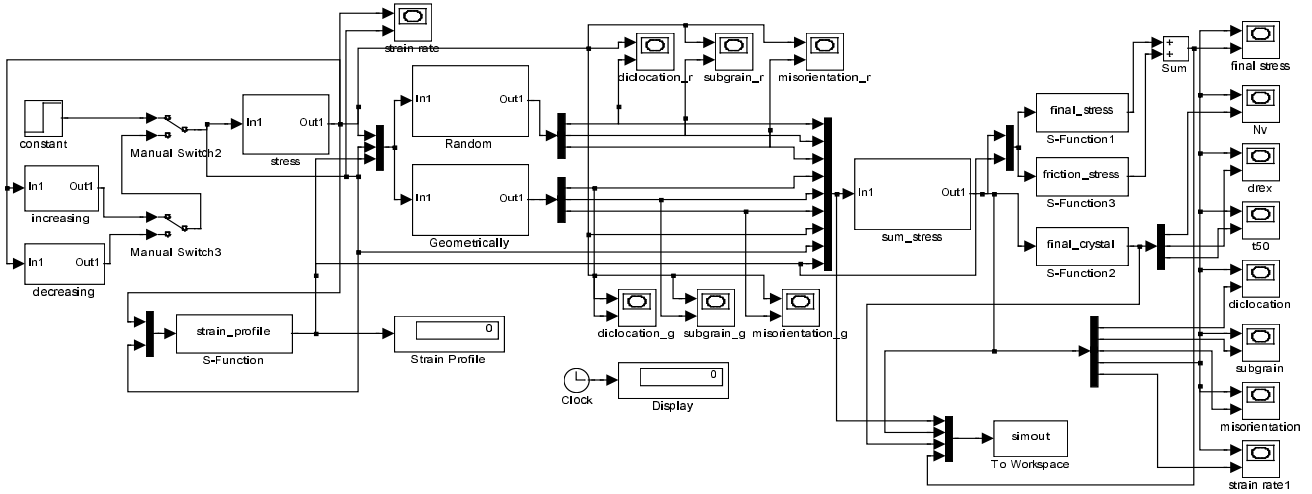


Fig. 12. Simulation diagram in SIMULINK of the microstructure grey-box model.

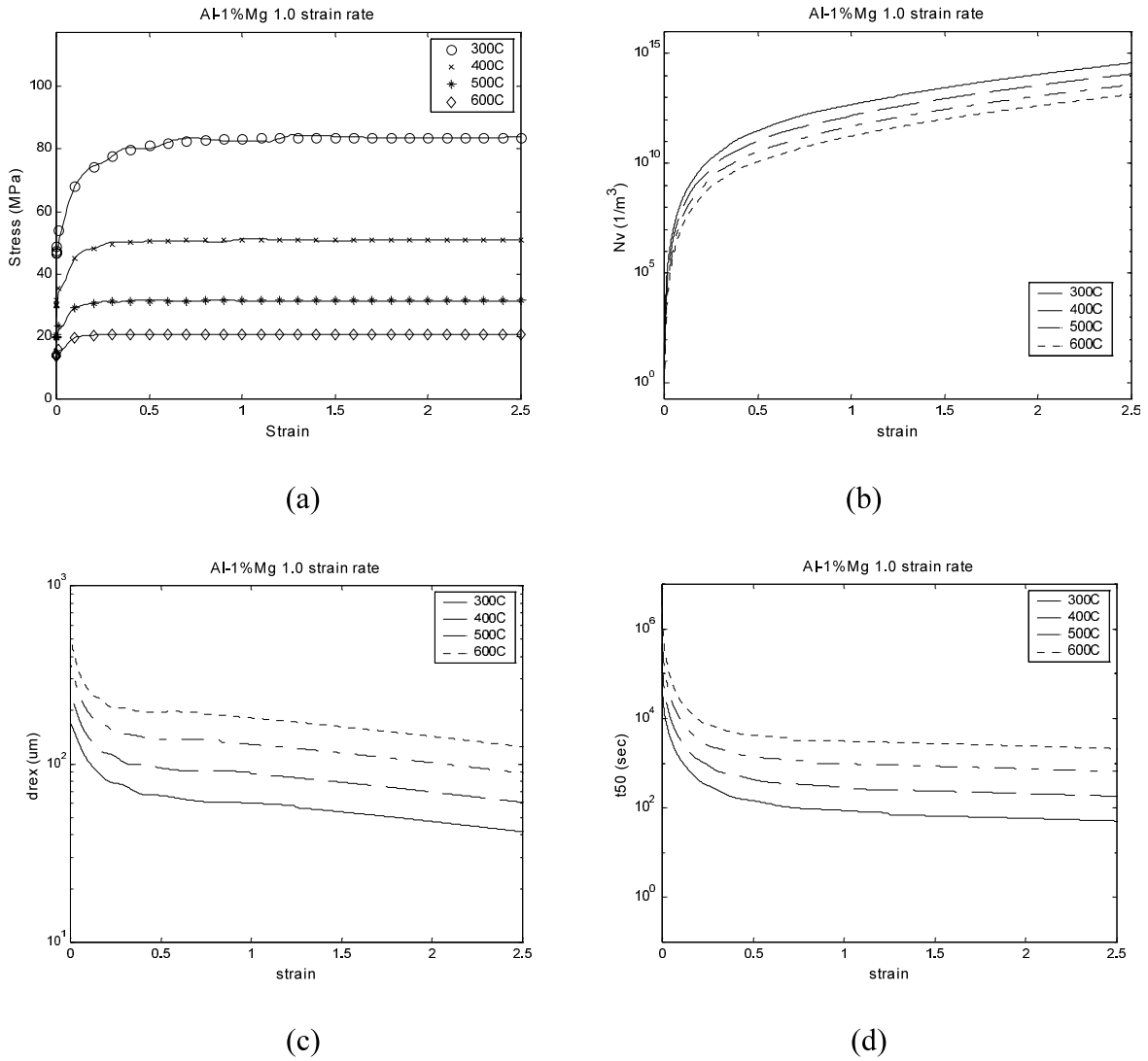


Fig. 13. Simulation results for Al–1% Mg microstructure evolution: (a) final flow stress; (b) nucleation density; (c) recrystallisation; and (d) 50% recrystallisation time.

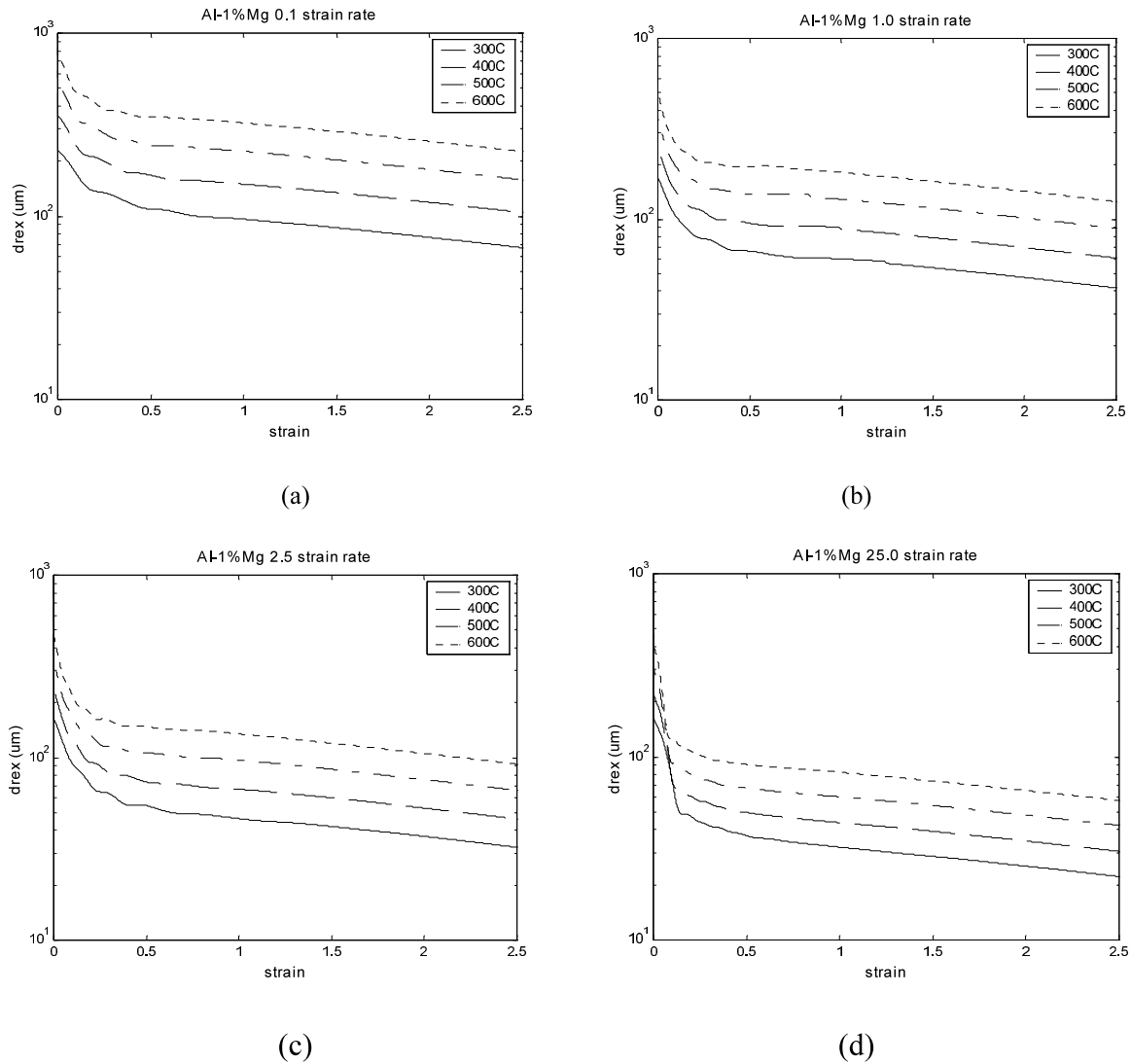


Fig. 14. d_{rex} curves for Al–1% Mg at different strain rates: (a) 0.1 s^{-1} ; (b) 1 s^{-1} ; (c) 2.5 s^{-1} ; and (d) 25 s^{-1} .

References

- [1] H.U. Löffler, D. Gade, R. Döll, H. Muller, T. Peuker, G. Sörgel, IFAC Workshop, Future Trends in Automation in Mineral and Metal Processing, Finland, 22–24 August 2000, p. 410.
- [2] C.M. Sellars, Q. Zhu, Mater. Sci. Eng. A280 (2000) 1.
- [3] H.J.A. Tulleken, Automatica 29 (1993) 285.
- [4] T. Bohlin, Automatica 30 (1994) 307.
- [5] M. Thompson, M. Kramer, 40 (1994) 1328.
- [6] D.A. Linkens, S. Kandiah, Trans. IChemE 74 (1996) 77.
- [7] L.A. Zadeh, Inform. Control 8 (1965) 338.
- [8] C.M. Sellars, in: B. Hutchison et al., (Ed.), Proceedings of the International Conference on Thermomechanical Processing, Theory, Modelling and Practice [TMP]², Stockholm, September 1996, The Swedish Society for Material Technology, 1997, p. 35.
- [9] C.M. Sellars, in: T.r. McNelley, (Ed.), 3rd International Conference on Recrystallisation and Related Topics, Monterey, California, USA, 21–42 October, Institute of Advanced Studies, 1996, p. 81.
- [10] Q. Zhu, H.R. Shercliff, C.M. Sellars, in: T. Chandra, T. Sakai (Eds.), Proceedings of the International Conference on Thermomechanical Processing of Steel and other Materials (THERMEC'97), Wollongong, Australia, July 1997, TMS, Warrendale, PA, 1997, p. 2039.
- [11] Q. Zhu, C.M. Sellars, in: J.H. Beynon et al. (Eds.), Proceedings of the 2nd International Conference on Modelling of Metal Rolling Processes, The Institute of Materials, London, 1996, p. 158.
- [12] G.J. Baxter, T. Furu, Q. Zhu, J.A. Whiteman, C.M. Sellars, Acta Mater. 47 (1999) 2377.
- [13] Q. Zhu, W. Blum, H.J. McQueen, Mater. Sci. Forum 217–222 (1996) 1169.
- [14] G.J. Baxter, Q. Zhu, M. Sellars, in: T. Sato et al. (Eds.), Proceedings of the 6th International Conference on Aluminium Alloys, their Physical and Mechanical Properties (ICAA-6), July 1998, Toyohashi, Japan, The Japan Institute of Light Metals, 1998, p. 1233.
- [15] H.E. Vatne, T. Furu, R. Orsund, E. Nes, Acta Mater. 44 (1996) 4463.
- [16] E.E. Underwood, Quantitative Stereology, Addison–Wesley, London, 1970.
- [17] J.H. Holland, SIAM J. Comput. 2 (1973) 89.
- [18] M.F. Abbod, M. Mahfouf, D.A. Linkens, Multi-Objective Genetic Optimisation for Self-Organising Fuzzy Logic Control, CONTROL'98, (vol. 2), University of Wales, Swansea, September 1–4, IEE, p. 1575.